Enhanced Fluorescence of Epicocconone in Surfactant Assemblies as a Consequence of Depth-Dependent Microviscosity

Debashis Panda, Saumyakanti Khatua, and Anindya Datta*

Department of Chemistry, Indian Institute of Technology Bombay, Powai, Mumbai 400 076, India

Received: August 13, 2006; In Final Form: November 15, 2006

The extents of fluorescence enhancement of epicocconone are found to be different in the micelles of the surfactants sodium dodecyl sulfate (SDS) and Triton X100 (TX 100). A decrease in fluorescence, observed in the cationic cetyltrimethylammonium bromide (CTAB) micelles, is rationalized by the formation of anions of the fluorophore at the Stern layer. To understand the difference in the effects of SDS and TX 100, the nature of the excited-state process in the fluorophore has been investigated by fluorescence spectroscopy, supported by complementary quantum chemical calculations. The excited-state dynamics of epicocconone is found to depend on polarity and viscosity of the medium, with a more pronounced dependence on viscosity. An inspection of the molecular orbitals involved in the electronic absorption of the molecule reveals the possibility of photoisomerization, which conforms to the observed solvent dependence of the fluorescence spectral properties. An apparent mismatch between trends observed in steady-state spectra and those in temporal decays indicates a significant contribution of an ultrafast component, which cannot be detected in the time resolution of our instrument. The viscosity dependence of the fluorescence quantum yields provides an explanation for the difference in the extents of fluorescence enhancement in the two micelles, in the light of location of the fluorophore at different depths of the micelle. The enhancement of fluorescence, with an unchanged fluorescence maximum, opens up the possibility that the fluorophore could be a useful dual emitting marker for fluorescence microscopy of heterogeneous systems, as the fluorescence of protein-bound epicocconone has been previously reported to be significantly red-shifted.

Introduction

In recent times, there has been considerable interest in fluorophores derived from biological sources.[1,2] Epicocconone (Figure 1) is one such fluorescent, cell permeable natural product isolated from the fungus *Epicoccum nigrum*. It is characterized by a high molar absorptivity ($\sim 10^4$) in wavelengths provided by common lasers, strong fluorescence in certain media, and a marked Stokes' shift of 100 nm between the absorption and emission maxima.[2] These properties make it a potentially good fluorescent probe for biotechnological applications like cell tracking[3] and two-color staining, when multiplexed with other fluorescent probes which have similar absorbances but different regions of emission.[4] Notably, epicocconone is only weakly fluorescent in aqueous solutions but becomes strongly fluorescent with an emission maximum at 610 upon addition of proteins like bovine serum albumin (BSA). This makes it an attractive fluorescent sensor for proteins, especially as it allows for the detection of proteins in as minute amounts as 100 pg/band, which is comparable to the limit of sensitivity of currently used fluorescent stains like SYPRO Ruby.[5] The enhancement of fluorescence of epicocconone in proteins has been proven to be due to the covalent binding of the compound to the N-terminii of the protein.[6]

In this article, we explore the possibility of enhancement of the fluorescence of epicocconone by noncovalent interaction with surfactant assemblies. The motivation for this study has its origin in the amphiphilic nature of the fluorophore, the structure of which comprises a heterocyclic fused ring system attached to a hydrocarbon tail and two polar hydroxyl groups (Figure 1). Such structural features are likely to enable epicocconone to bind noncovalently with membranes and surfactant assemblies, thereby causing an enhancement of fluorescence, as has been observed for other fluorophores.[7,8] To investigate this phenomenon, we have performed fluorescence monitoring of its interaction with micelles and reverse micelles, which are the simplest mimics of membranes. We have also addressed the issue of protonation/deprotonation of the ionizable side chain at the interface of water and the surfactant assemblies, which can affect the ground- and excited-state equilibria of fluorophores considerably.[9,10] The objective of this study is to understand whether the fluorescence properties of epicocconone in membranelike systems are the same as or different from those of the protein-bound fluorophore, for if they are indeed different from each other, then the fluorophore would be particularly attractive as a probe for imaging, as it could be capable of differentiating between these two kinds of cellular components, thereby eliminating the need of its multiplexing with other fluorophores to some extent.

Materials and Methods

Deep purple total protein stain from Amersham Biosciences, which contains epicocconone as the active ingredient, is used as received. Micromolar concentrations of the fluorophore have been maintained in all experiments. Deionized water is distilled twice before being used as a solvent. *n*-Heptane of spectroscopic grade from Spectrochem, India, is distilled over calcium hydride immediately prior to use. The surfactants Triton X-100 (TX 100), cetyltrimethylammonium bromide (CTAB), sodium dode-

* To whom correspondence should be addressed. E-mail: anindya@chem.iitb.ac.in. Phone: +91 22 2576 7149. Fax: +91 22 2572 3480.

10.1021/jp065226o CCC: $37.00
Published on Web 01/31/2007

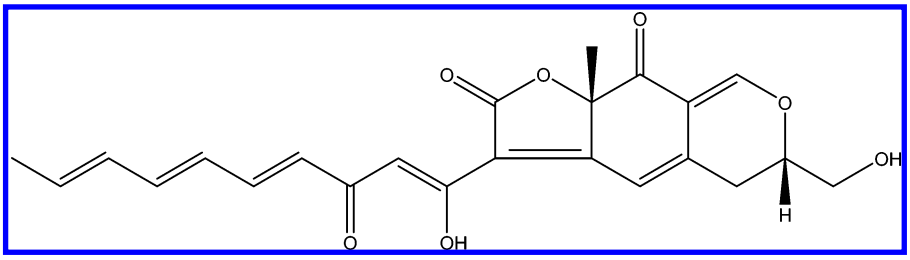

Figure 1. Molecular structure of epicocconone.

cyl sulfate (SDS), and Aerosol OT (AOT, sodium bis(2-ethyl-1-hexyl)sulfosuccinate) are obtained from Aldrich. The first three surfactants are used as received, whereas AOT is mixed with 1:20 w/w activated charcoal powder, dissolved in methanol, and stirred overnight, followed by evaporation of the solvent in a rotary evaporator. The absorption and fluorescence spectra are recorded on a JASCO V 530 spectrophotometer and Perkin-Elmer LS55 fluorometer, respectively. The excitation wavelength (λ_{ex}) is 430 nm. The absorbance at this wavelength is kept below 0.1 to avoid inner filter effects. Fluorescence quantum yields (ϕ_f) are calculated after proper correction for changes in absorbance using Lucifer yellow CH ($\phi_f = 0.21$) as the reference.[11] Synchronous fluorescence studies have been performed by scanning the excitation and the emission monochromators of the fluorometer simultaneously, with a constant offset of 20 nm between the two. The resonance light scattering spectra are obtained similarly but with a zero offset. Time-resolved fluorescence measurements are performed at the magic angle using a picosecond pulsed diode laser based TCSPC fluorescence spectrometer with $\lambda_{ex} = 406$ nm from IBH, U.K. The emission from the samples at 530 nm is collected at a right angle to the direction of the excitation beam. The full width at half-maximum of the instrument response function is 250 ps, and the resolution is 7 ps/channel. The data are fitted to multiexponential functions after deconvolution of the instrument response function by an iterative reconvolution technique, using the IBH DAS 6.0 data analysis software, where reduced χ^2 and weighted residuals serve as parameters for goodness of fit.[12]

The ground-state geometries are optimized using the density functional theory method with the Becke3LYP functional[13,14] as implemented in the Gaussian 03 software package.[15] The default options for the self-consistent field (SCF) convergence and threshold limits in the optimization are used. First, time-dependent density functional theory (TDDFT) calculations are performed on the gas-phase-optimized geometry of the ground state (S0).[16,17] Vertical excitations are carefully analyzed by inspecting the corresponding Kohn−Sham orbital contours generated with MOLDEN program.[18] Next, long-range effects induced by solvent polarity on the predicted photophysical properties are taken into account by means of dielectric continuum approach using the polarizable continuum model (PCM).[19]

Results and Discussion

Fluorescence Studies in Surfactant Assemblies. The absorption spectra in TX 100 and SDS micelles exhibit no considerable shift in maximal wavelengths compared to that in the neat aqueous solution, whereas, in CTAB, the maximum at 430 nm gives way to a new one at 560 nm (Figure 2a). This indicates a change in the ground state of the fluorophore in the presence of the cationic CTAB micelles, which is ususally explained by a protonation/deprotonation of the fluorophore at the Stern layer, due to an altered local pH in this region.[9,20,21] Another possible explanation could be in the form of the surfactant-induced aggregation of the fluorophore, especially in the anionic form, due to electrostatic interaction with the oppositely charged headgroups. However, such dye−surfactant aggregates are generally formed in submicellar concentrations and get disrupted above the critical micellar concentration (cmc).[22,23] So, we suspect that the new, red-shifted absorption band is that of the anion, formed in the Stern layer of CTAB micelles. It may be mentioned here that a red shift in the absorption maximum has been observed upon deprotonation of several dyes, the most notable of them being phenolpthalein. This contention is further explored by fluorescence studies in micellar and neat aqueous media as well as quantum chemical calculation.

Epicocconone has two excitation maxima, as reported by Karuso and co-workers.[5] The fluorescence intensity increases upon addition of all the three surfactants, up to the respective values of the critical micellar concentration (cmc). Subsequently, it reaches a saturation value in TX 100 and SDS, whereas a decrease is observed with CTAB (Figures 2b and 3). The increase in fluorescence quantum yield in the neutral TX 100 and the negative SDS micelles can be due to two reasons. First, when the fluorophore resides in the apolar cores of the micelles, the more fluorescent apolar excited states are populated to a greater extent than the polar excited states, which are usually less fluorescent.[24,25] Besides, water is a good quencher for many fluorophores, due to specific interaction. The fluorophore is protected from such quenching upon sequestering in micelles.[26] Another reason could be the existence of aggregates of the fluorophore in water and their disruption upon micellization. Generally, the aggregates are nonfluorescent and the micellized monomers are highly fluorescent. A third alternative explanation could be in the existence of excited-state heterogeneity arising from an excited-state process that might be operative in the fluorophore. It is possible that the emissive excited state is

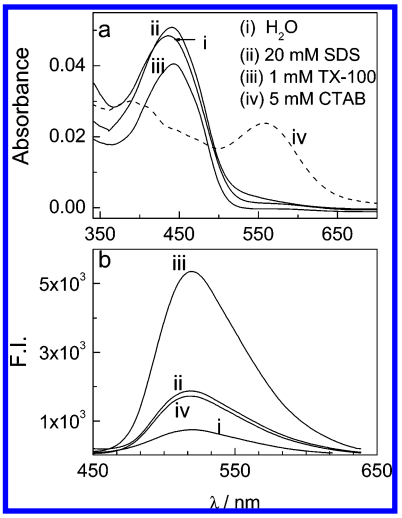

Figure 2. (a) Absorption and (b) fluorescence ($\lambda_{ex} = 430$ nm) spectra of 2 μL/mL of epicocconone in aqueous solutions containing (i) no surfactant, (ii) 20 mM SDS, (iii) 1 mM TX 100, and (iv) 5 mM CTAB.

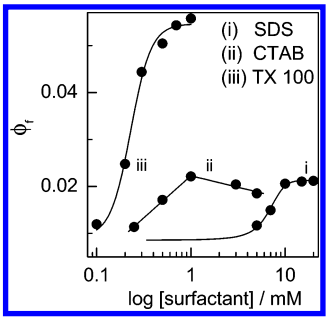

Figure 3. Variation of fluorescence quantum yield of epicocconone in aqueous solution (2 μL/mL), with the concentration of (i) SDS, (ii) CTAB, and (iii) TX 100 (λ_{ex} = 430 nm).

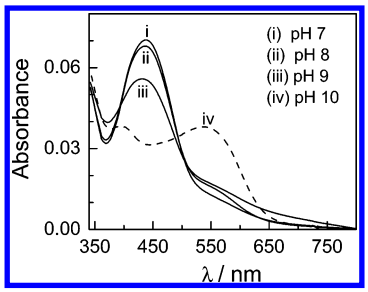

Figure 4. Absorption spectra of epicocconone in aqueous solutions of varying acidity (pH = (i) 7, (ii) 8, (iii) 9, and (iv) 10).

formed to a greater extent in micellar media. Concentration dependence of the fluorescence spectra has been studied, in addition to dynamic light scattering experiments, to ascertain whether aggregates are present or not. Time-resolved fluorescence studies have been performed to explore the excited-state dynamics. Before we describe them, however, the fluorescence spectra in CTAB micelles warrant a closer inspection.

It has been mentioned already that from the absorption spectroscopic studies, we suspect that an anionic form of the fluorophore is formed in CTAB micelles. As is shown in Figure 4, a red-shifted absorption band occurs at 550 nm, identical with that in CTAB, appears as the pH is changed from 7 to 10. Thus, the contention about formation of the anion in the Stern layer of the CTAB micelles gains some support. Upon excitation at 550 nm, no fluorescence emission is observed from the homogeneous aqueous solution of epicocconone at pH 10, indicating that the anion is nonemissive. The 560 nm excitation of epicocconone in the 7 mM CTAB micellar solution yields no emission either. This lends further credence to the argument about formation of the anion in the micelle and also provides an explanation for the decrease in the fluorescence intensity in CTAB solutions, post-cmc, in the light of a decrease in the number of emitting species (i.e., the number of neutral epicocconone molecules) due to the formation of the nonfluorescent anion in these conditions. As this effect is absent in SDS and TX 100, the fluorescence intensity reaches a plateau in these surfactants.

Before indulging in a discussion about the excited-state dynamics, it is imperative to investigate the possibility of ground-state heterogeneity of the fluorophore. This is performed conveniently through synchronous fluorescence experiments.[27−29] In this experiment, the excitation and emission wavelengths are varied simultaneously with a constant offset, which is chosen by trial and error, so that the experiment is performed along the diagonal of the excitation−emission matrix, which passes through the maximum number of peaks and troughs. The resulting spectra have a greater number of bands compared to that obtained in conventional absorption−excitation spectra, and

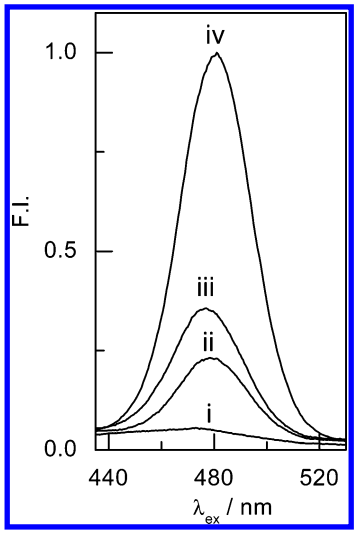

Figure 5. Synchronous fluorescence spectra of epicoccocone in aqueous solution (2 μL/mL) containing (i) no surfactant, (ii) 5 mM CTAB, (iii) 20 mM SDS, and (iv) 1 mM TX 100. The wavelength offset is 20 nm, and the bandpass is 5 nm.

this allows a better recognition of fluorophores present together in the solution. This method has previously been utilized to analyze complex mixtures in as widely separated fields as cancer diagnosis,[27] hydrocarbon analysis in mineral oils,[28] and the study of mitochondria.[29] In the present experiment, the synchronous fluorescence spectra of epicocconone exhibit a single peak at 480 nm in all the three micelles (Figure 5). This indicates the presence of a single emissive ground-state species in these media. The trend of variation of the intensity is similar to that observed in the regular fluorescence spectra. Initially, the intensity increases quite sharply with the addition of surfactant and then gets saturated at higher surfactant concentrations.

Bimodal Decay of Fluorescence. An analysis of the fluorescence decay traces (Figure 6) reveals the presence of two components: a short one with a lifetime of 0.25 ns and a longer one of 1.1 ns (Table 1). The shorter lifetime does not change considerably upon addition of surfactants, but that of the longer one decreases gradually. In TX 100 and CTAB, the relative amplitude of the longer lifetime increases and that of the shorter component decreases progressively with the addition of surfactant. The amplitudes change to a lesser extent in the anionic SDS than in the neutral Triton X100. These results provide a substantial rationalization of the steady-state fluorescence data. The presence of the two components signifies the existence of two different species. The absence of change of the 250 ps lifetime could indicate that the species associated with it remains predominantly in the aqueous phase. The decrease in its relative contribution upon addition of the surfactants indicates that its concentration decreases upon incorporation in micelles, with a concomitant increase in the concentration of the species with the longer lifetime. The decrease in the magnitude of the longer lifetime possibly indicates some quenching by the micelles. However, the increase in the abundance of the species with longer lifetime explains the increase in quantum yield of epicocconone upon incorporation in SDS and TX 100 micelles. At this point, the question that arises is regarding the nature of the two species involved. The structure of epicocconone (Figure 1) is somewhat like that of a surfactant. So, it is possible that it exists in aqueous solutions in the form of aggregates. Since the aggregates of fluorophores usually undergo self-quenching, it can be expected that such aggregates have a small fluorescence quantum yield and a short lifetime of 250 ps. In that case, the

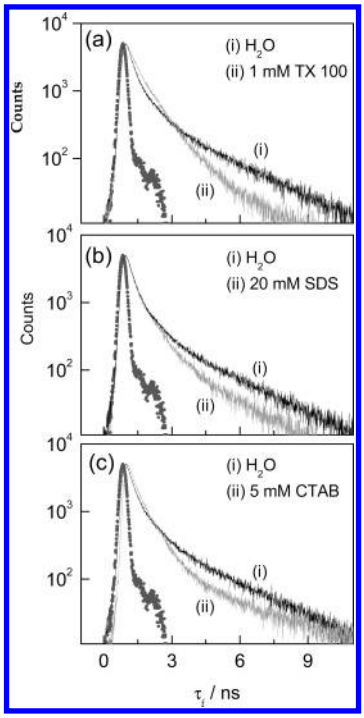

Figure 6. Fluorescence decays of epicocconone in different micelles: (a) TX 100; (b) SDS; (c) CTAB. The IRF is shown in the dashed line. $\lambda_{ex} = 406$ nm, and $\lambda_{em} = 530$ nm.

TABLE 1: Fluorescence Decay Parameters of Epicocconone in Different Micelles

micelle	concn of surfactant	τ_1/ns	τ_2/ns	a_1	a_2	χ^2
TX 100	0	0.25	1.11	0.80	0.20	1.08
	0.1	0.23	0.99	0.77	0.23	1.09
	0.2	0.25	0.89	0.61	0.39	1.02
	0.3	0.28	0.91	0.55	0.45	1.09
	0.5	0.23	0.85	0.52	0.48	1.10
	0.7	0.28	0.92	0.53	0.47	1.08
	1.0	0.25	0.88	0.50	0.50	1.18
CTAB	0	0.25	1.13	0.80	0.20	1.13
	0.25	0.28	1.28	0.75	0.25	1.01
	1.00	0.24	0.89	0.62	0.38	1.06
	3.00	0.26	0.83	0.62	0.38	1.14
	5.00	0.17	0.70	0.57	0.43	1.20
SDS	0	0.25	1.13	0.80	0.20	1.04
	5	0.25	1.04	0.76	0.24	1.15
	10	0.25	0.98	0.80	0.20	1.14
	15	0.25	0.88	0.73	0.27	1.17
	20	0.26	0.79	0.72	0.28	1.00

longer lifetime would be assigned to monomers of the fluorophore. Upon addition of the surfactants, the aggregates of the fluorophore are expected to get disrupted and micellized. This would give rise to an increase in the relative population of the longer component, which is exactly what we have observed. The decrease in the magnitude of the component could be explained by quenching of the micellized monomer by surfactant molecules in the micelles. The hypothesis on aggregation is seemingly vindicated in the he steady state and time dissolved study of epicocconone in AOT reverse micelles in *n*-heptane. The choice of this study is motivated by the fact that, in the AOT/*n*-heptane system, the aggregates of the fluorophore are not likely to exist. So, we can expect a large fluorescence quantum yield and the absence of the 250 ps component of the lifetime. Indeed, we have observed a considerably enhanced fluorescence quantum yield of 0.24 in AOT/heptane solutions without water (Figure 7a). The fluorescence quantum yield falls off upon the gradual addition of water, to a saturation value of

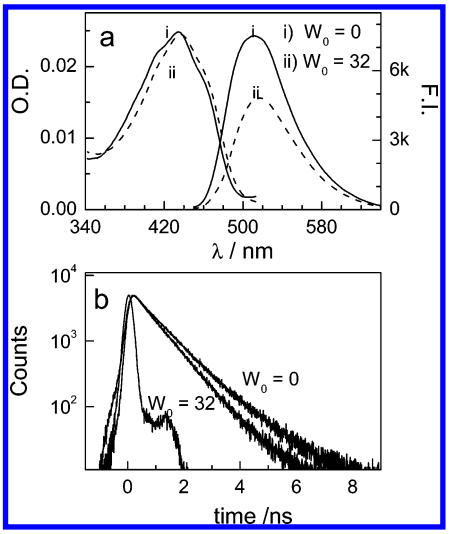

Figure 7. (a) Absorption and fluorescence spectra and (b) the fluorescence decay traces of epicocconone in AOT reverse micelles. $\lambda_{ex} = 430$ nm in (b); $\lambda_{ex} = 406$ nm and $\lambda_{em} = 530$ nm in (c).

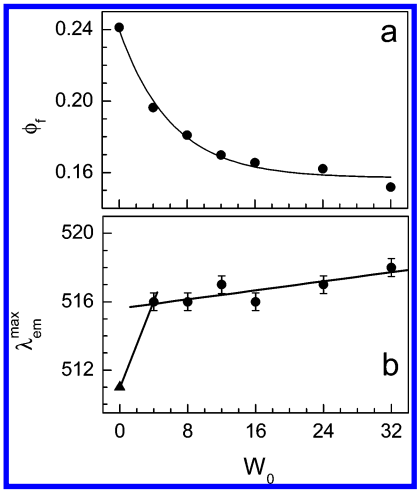

Figure 8. (a) Variation of the emission maximum and (b) change in fluorescence quantum yield with the water content of AOT microemulsions.

TABLE 2: Decay Parameters of Epicocconone in Reverse Micelles

W_0[a]	τ/ns	χ^2	W_0[a]	τ/ns	χ^2
0	0.95	1.11	16	0.87	1.18
4	0.96	1.04	24	0.85	1.30
8	0.90	1.03	32	0.83	1.10
12	0.88	1.04			

[a] W_0 = no. of moles of water/no. of moles of AOT.

0.15 in $W_0 = 24$. The emission maximum (λ_{max}) gets red-shifted by 10 nm (Figure 8b). The time-resolved fluorescence decays in AOT reverse micelles exhibits only one component with a life time around 1 ns. Upon addition of water the lifetime of this component decreases very slowly (Figure 7b, Table 2). Thus, the absence of the 250 ps component conforms with the proposed model. In AOT, the fluorophore can be expected to exist solely as monomers, the fluorescence of which is quenched upon addition of water.

Breakdown of the Hypothesis on Aggregates. To ascertain the viability of the model proposed above, we have investigated the concentration dependence of the fluorescence spectra of epicocconone. If aggregation is really the origin of the bi-exponential decay of epicocconone, then one might expect the

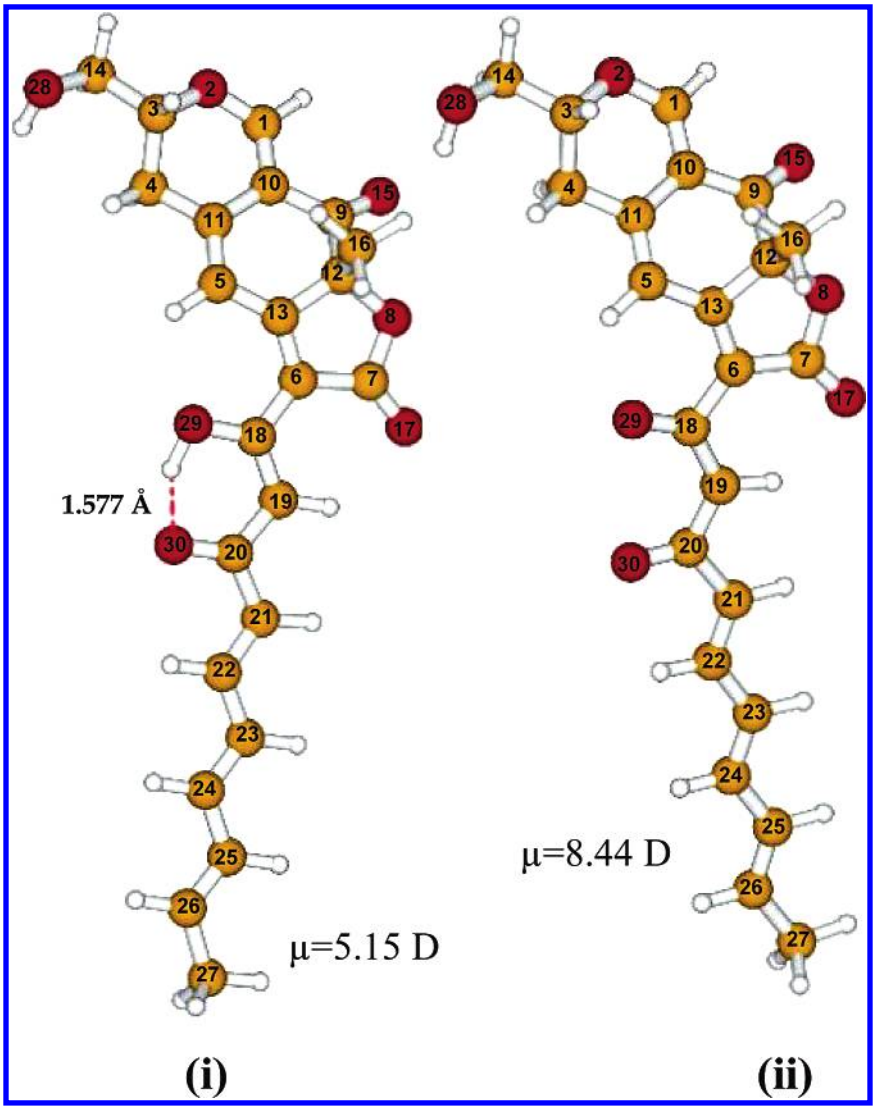

Figure 9. B3LYP/6-31G*-optimized geometries of (i) neutral and (ii) anion forms of epicocconone.

contribution of the longer component to decrease and that of the shorter component to increase upon increasing the concentration of the fluorophore. The fluorescence quantum yield is also expected to decrease upon increasing the concentration. However, we find that the shape of the absorption spectrum remains unchanged upon increasing the concentration of the fluorophore (Figure S3a). The emission spectra at different concentrations, normalized by the intensity of the light absorbed, are also found to be identical with each other (Figure S3b). The fluorescence decay traces are superimposable in this concentration range (Figure S3c). Thus, we can conclude that aggregation is not the origin of the bimodal fluorescence decay, provided it can be shown that the fluorophores actually aggregate in the range of concentrations used in this experiment. This is tested by performing resonance light-scattering experiments.

In general, in the spectral range where a solution has optical absorption, an increase in scattered light intensity can be observed as a result of the increase of refractive index of the scattering medium in this range (RLS effect).[30] Usually this increase is masked by absorption; however when aggregates are formed, this effect can be strong enough since the RLS intensity is proportional to the square of volume of the scattering particle. Thus, RLS has become an important tool for testing for the formation of aggregates.[30,31] Even though there is no RLS signal at 1.5 μL/mL of epicocconone, a band is found to develop as the concentration is increased to 12 μL/mL, indicating aggregation in this range (Figure S3d). However, it has been mentioned in the last paragraph that the fluorescence quantum yields as well as lifetimes do not change over this range. Thus, we can conclude that aggregation is not responsible for the shorter component of fluorescence. Rather, some fast nonradiative process is likely to be operative. To obtain a clearer picture of the structural aspects, which are likely to play an important role in the excited-state process, we have performed quantum chemical calculations, as is described in the next section.

Quantum Chemical Calculations. The two primary objectives for performing the quantum chemical calculations are to justify the red shift in the absorption spectrum of the anion and to gain an insight to the excited-state dynamics of the fluorophore, which is the first step to understand the origin of the enhancement of fluorescence in micelles. Full geometry optimization of both the forms (neutral and anionic) of epicocconone has been carried out independently at the B3LYP/6-31G* level of theory. The optimized structure of the neutral form is depicted in Figure 9. That for the anion is shown in Figure S1. The dipole moments of the neutral and anionic forms have quite high values of 5.15 and 8.44 D, respectively. The key structural parameters, especially bond angles and dihedral angles, are summarized in Table S2. The hydrogen atom bonded with O29 is within the

TABLE 3: Important Vertical Excitations Computed at the TDDFT/B3LYP/6-31+G*//B3LYP/6-31G* Level for Epicocconone

	parent		anion	
param	energy (nm)	oscillator strength	energy (nm)	*oscillator strength*
		Gas Phase Computed Data		
ES 1[a]	467.65	1.0685	734.76	0.1892
ES 2	401.89	0.5248	699.02	0.0217
ES 3	386.88	0.0000	614.85	0.1861
		Condensed Phase (Water)[b] Computed Data		
ES 1	486.95	1.4583	514.19	0.7561
ES 2	413.91	0.2791	466.59	0.0020
ES 3	363.74	0.0179	425.65	0.0491
		Experimental Data[c]		
$^{abs}\lambda_{max}$ in nm	438 (water)		545 (pH 10)/570 (5 mM CTAB)	

[a] ES stands for excited state. [b] Calculated using the PCM//B3LYP/6-31+G*//B3LYP/6-31G* level. [c] Experimental condition is given in parentheses.

hydrogen-bonding distance of O30 (1.577 Å) (Figure 9). It is this enolic hydrogen atom that is lost during deprotonation in basic media, leading to a more or less equal distribution of the consequent negative charge on the two oxygen atoms, as is evident in Muliken charges of −0.593 and −0.565 on O29 and O30, respectively, in anionic form, computed at the B3LYP/6-31G* level of theory. Such a deprotonation is expected to lead to a structural change as the unsaturated tail of the epicocconone comes closer to the cyclic rings as a consequence of electrostactic repulsion between the partially negatively charged oxygen atoms (O29, O30).

The vertical excitations of the neutral and the anionic forms of the fluorophore have been computed using the time-dependent density functional theory (TDDFT) with B3LYP functional on the optimized geometries of singlet ground states of the two species, as TDDFT generally predicts results that are closer to the experimental findings for large systems than Hartree−Fock-based CIS. The polarizable continuum model (PCM) has been considered for computation of excitation energy of epicocconone in the condensed phase of water. Highest intensity transitions in the lower energy region of epicocconone are listed in Table 3, along with the corresponding experimental data. A good qualitative agreement in trends of spectral shifts is found between the two sets. In the anionic form, the λ_{max} is predicted to be red-shifted from that of the neutral form by 27 nm in water whereas a red shift of 267 nm is computed in the gas phase. Such red shifts are likely to be due to a greater amount of conjugation in the anionic form, the localized electronic charge on the ground state of which gets dissipated over the molecule upon electronic excitation.

Experimentally, a red shift of 107 nm is observed in aqueous solution and a further red shift of 25 nm is observed in CTAB, as has been mentioned already. This is in qualitative agreement with the computational result of a greater red shift in more apolar media, of which the gas phase is an extreme example. The quantitative dissimilarity of computed and observed red shifts of λ_{max} between the normal and anionic forms of epicocconone in the lower energy region can be primarily ascribed to two factors. TDDFT does not account for specific solvent−solute interactions such as H-bonding of water with epicocconone. Besides, the micropolarity of CTAB is much more than that of the gas phase, even though it is significantly less than that of water. So, the red shift in CTAB micelles is expected to be somewhere between the values predicted in water and the gas phase. This is indeed observed experimentally.

A possible reason for the red shift in the absorption spectrum, expected from the computational results and observed experimentally, can be provided upon a closer investigation of the Kohn−Sham orbital contours for the frontier MOs (Figure 10).

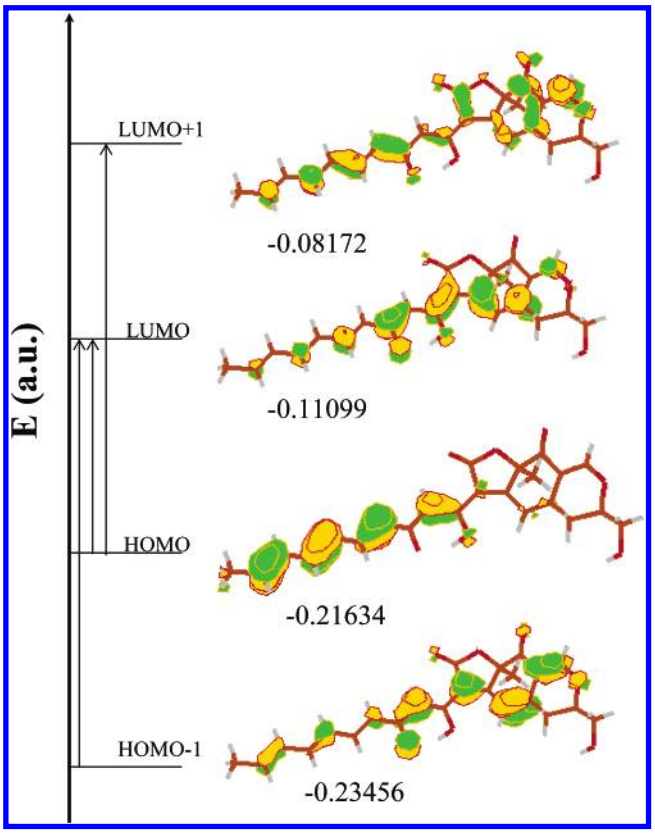

Figure 10. Kohn−Sham orbital contours involved in the key vertical excitations computed at the TDDFT/B3LYP/6-31+G*/CPCM//B3LYP/6-31G* level for the neutral form of epicocconone.

The highest occupied energy level (HOMO) is found to predominantly of π-character and is localized on the side chain. On the other hand, the antibonding lowest uncoccupied molecular orbital (LUMO) is delocalized over the molecule. The most intense transition is found to be of $\pi-\pi^*$ type, predominantly between the HOMO and the LUMO. Thus, a more uniform charge distribution over the molecule is expected in its first excited state as compared to the ground state, as the electron density moves from an orbital localized on the chain to one that is more delocalized. So, the first excited state is expected to be less polar than the ground state, implying that the difference in energies of these two states should be greater in polar media compared to apolar ones, as the polar ground state would be stabilized to a greater extent than the apolar excited state. In other words, a red shift in the absorption maximum can be expected upon decreasing the polarity of the medium.

The Kohn−Sham orbital contours also provide some insight into the possible excited-state process that is operative in

epicocconone. The migration of π-electron density away from the chain, upon photoexcitation, causes a decrease in the π bond order of the chain, making it a candidate for photoisomerization. Since this excited-state process involves a change in conformation of the chain, it is possible that it is suppressed in micelles, and this could be a cause of an increase in the fluorescence quantum yield and contribution of the 1 ns component. In that case, the 250 ps component should be assigned to the photoisomer. A considerable amount of literature exists on similar hindrance of photoisomerization in micelles, mainly ascribed to their high microviscosity.[32,33]

Of course, one cannot rule out the possibility of other excited-state processes at this point. The proximity of the hydrogen atom bonded to O29 to O30, for example, makes the molecule a candidate for an excited-state proton transfer (ESPT). It is imperative to look into the occurrence of one or both of these photoprocesses by further experiments. So, we have investigated the effect of isotope substitution as well as changing the viscosity of the medium on the excited-state characteristics of epicocconone. The results of these experiments are discussed in the following section.

Effects of Deuteration and Viscosity. A rather slender variation in the fluorescence maximum and the fluorescence quantum yield is observed upon changing the solvent from H_2O to D_2O (Figure 11a). The variation in the temporal features is more remarkable (Figure 11b, Table 4). Whereas the relative amplitudes remain constant, the lifetimes are found to get doubled in D_2O. Such an isotope effect is often interpreted as an evidence of ESPT,[12,34] but it is not conclusive evidence, as there have been several reports of ESPT, where the isotope effect is not observed[35] and, then again, the isotope effect is often observed for other photoprocesses as well.[36] Besides, the isotope effect observed here is pretty small, which is usually not the case with ESPT. On the other hand, viscosity has a rather profound effect on the fluorescence quantum yield (Figure 11a), as a 5-fold increase is observed from water to *tert*-butanol. As a control experiment, the fluorescence quantum yield has been measured in an acetonitrile solution. The value of quantum yield observed in this experiment is 0.024, which is much greater than that in aqueous solutions (0.008) but is significantly lesser than that in *tert*-butanol (0.047). This implies that the photophysics of epicocconone has a strong viscosity dependence, as the polarities of *tert*-butanol and acetonitrile are almost the same (the empirical micropolarity parameter, $E_T(30)$,[37] being 43.3 and 45.6, respectively), whereas *tert*-butanol is significantly more viscous than acetonitrile (4.45 and 0.38 mPa s, respectively).[38] Hence, we propose that the major nonradiative pathway in epicocconone involves photoisomerization, which requires conformational freedom, which in turn is lost to a greater extent in more viscous media. So, a medium of greater microviscosity causes a hindrance to the nonradiative process and increases the fluorescence quantum yield.

Surprisingly, the fluorescence decay appears to become faster in the more viscous organic solvent, where the quantum yield is greater. This is unexpected, as such a remarkable increase in fluorescence intensity accompanied by unaltered or decreased lifetimes would imply a drastic change in the radiative rate, which, despite being observed on solid an nanomolecular substrates, is not commonly observed in simple solutions.[39,40] The more feasible explanation can be offered in terms of a significant amount of ultrafast decay, which is not observed in the time resolution of our experiment. Such an ultrafast component would, nevertheless, have its signature in the steady-state fluorescence spectrum, in the form of a decrease in the fluorescence quantum yield. Tentatively, the 1 ns component is ascribed to the locally excited state that undergoes photoisomerization, as its contribution increases in micelles, where

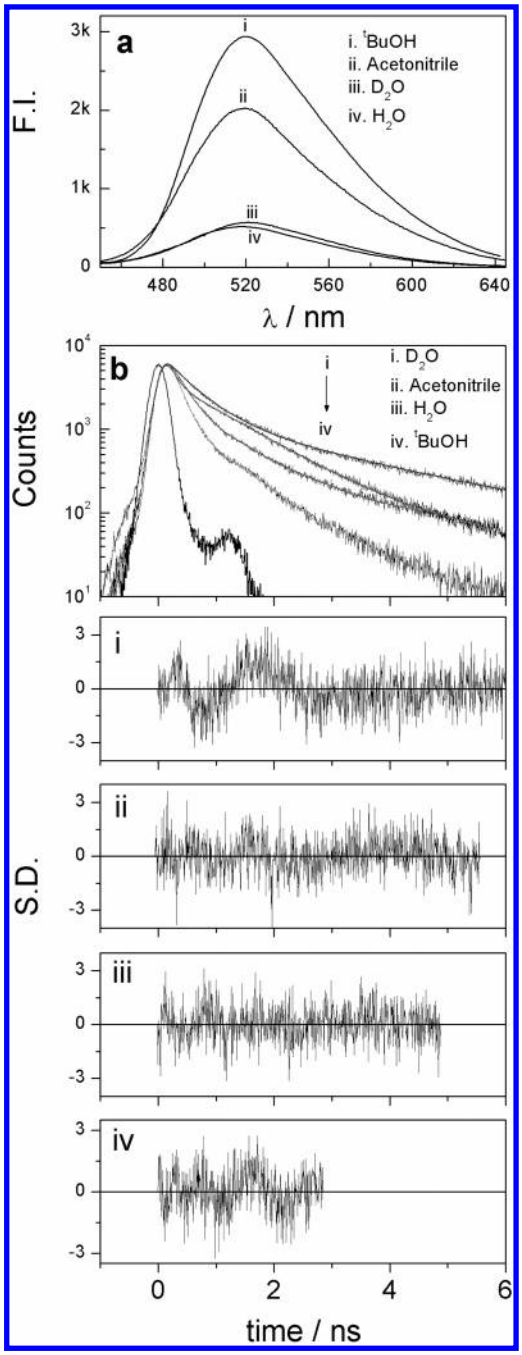

Figure 11. (a) Emission spectra of epicocconone in representative solvents: (i) *tert*- butanol; (ii) acetonitrile; (iii) D_2O; (iv) H_2O. λ_{ex} = 430 nm. (b) Fluorescence decays of epicocconone in representative solvents: (i) *tert*-butanol; (ii) acetonitrile; (iii) D_2O; (iv) H_2O. λ_{ex} = 406 nm, and λ_{em} = 530 nm. The solid lines denote the curves of the best fit. The IRF is shown in dashed lines. The weighted residuals are depicted below the fluorescence decays.

TABLE 4: Spectral and Temporal Parameters for Epicocconone in Representative Organic Solvents

solvent	φ_f	τ_1/ns	τ_2/ns	a_1	a_2	χ^2
dicholoromethane	0.028	0.20	0.94	0.20	0.80	1.03
acetonitrile	0.024	0.11	1.09	0.70	0.30	1.10
^{t}BuOH	0.047	0.18	1.11	0.91	0.09	1.15
H_2O	0.008	0.25	1.11	0.80	0.20	1.03
D_2O	0.009	0.51	2.62	0.82	0.18	1.20

the photoprocess is proposed to be retarded. The shorter component is likely to have contributions from the ultrafast nonradiative decay due to photoisomerization as well as the lifetime of the photoisomer, making the interpretation of the coefficient associated with it rather complicated.

Rationalization of the Difference in Fluorescence Enhancement in SDS and TX 100. The steady-state fluorescence results in the homogeneous solutions can be used to rationalize the different degrees of enhancement of fluorescence in Triton X 100 and SDS. The enhancement in these micelles is clearly due to the suppression of a nonradiative process, which can be ascribed to one or all of the following factors: sequestering from water, leading to a decrease in polarity and proticity of the microenvironment of the fluorophore, as well as a significant increase in the microviscosity. As the deuterium isotope effect is rather small, whereas the effect of decreasing the polarity is quite significant, the increase in fluorescence intensity in SDS compared to that in water is ascribed to a lower micropolarity experienced by the fluorophore in the micelle. However, the change in micropolarity does not explain the difference in the extents of fluorescence enhancement in TX 100 and SDS. The greater increase in fluorescence intensity in TX 100 implies that it experiences a higher microviscosity in TX 100 compared to that in SDS.[32,41,42] The greater microviscosity, evidently experienced by epicocconone in TX 100, is rationalized as follows: It has been reported that the Stern layer of SDS is only 6−9 Å thick, whereas the thickness of the palisade layer of TX 100 is 25−27 Å.[43,44] This is so because of the long hydrophilic headgroup present in TX 100. Thus, the region of the TX 100 micelle, just beneath the palisade layer, is expected to be associated with a greater degree of compactness and, consequently, a greater microviscosity than the corresponding region in SDS micelle that is just beneath the Stern layer. The variation of compactness of packing of the apolar chains with depth is a well-known phenomenon and has been demonstrated in the span of microviscosities, from a few to 150 cP, that is reported by fluorescent probes, depending on their extent of penetration in the micelle.[45,46] This forms the basis of depth-dependent analysis of lipid membranes.[47]

We propose that the fluorophore resides just inside the Stern layer/palisade layer. Since the inner boundary of the palisade layer in TX 100 is much deeper within the micelle, compared to that of the Stern layer of the SDS micelle, epicocconone is buried further inside the micelle in TX 100 and, therefore, experiences a significantly greater microviscosity in TX 100, due to a greater extent of packing of the surfactant chains (Chart 1). The decrease in fluorescence quantum yield in AOT reverse micelles is likely to be due to the increase in the extent of photoisomerization, caused by the decrease in the compactness of the alkyl chains, as the reverse micelles get "blown up" upon addition of water.

CHART 1: Proposed Location of Epicocconone, Represented as the Green Oval-Shaped Object, in the Two Micelles[a]

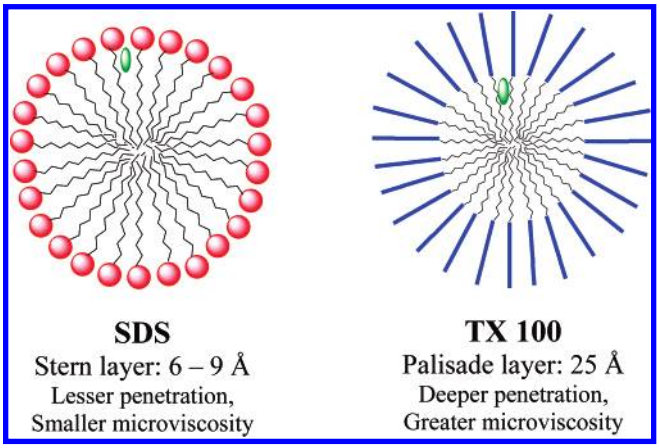

[a] The head groups of SDS and TX 100 are represented by red circles and thick blue lines, respectively, to denote the difference in their lengths. The difference in the extent of penetration of the fluorescent probe, due to the difference in the length of the headgroups and, consequently, the Stern layer/palisade layers, is proposed to be responsible for the difference in the extents of augmentation of fluorescence in the two micelles, as the microviscosity experienced by the fluorophore in TX 100 is expected to be much greater than that in SDS.

Conclusion

The apparently bimodal fluorescence decay of epicocconone in neat solutions is associated with an ultrafast decay, which is missed in the time resolution of our experiments. The ultrafast decay is likely to be due to photoisomerization, as a significant viscosity dependence of the fluorescence quantum yield is observed. The enhancement of the fluorescence intensity in micelles is ascribed to a decrease in the extent of this photoprocess due to a higher microviscosity. The difference in the extent of fluorescence enhancement in TX 100 and SDS is rationalized as an effect of a greater penetration of the fluorescent probe in case of the first micelle, which in turn is due to the difference in the thichness of the hydrophilic palisade/Stern layers of the two micelles.

The results of this study are likely to have implications in biophysical applications of the fluorophore. The lifetimes associated with it are found to be 250 ps and 1 ns, respectively. Thus, when using the protein stain for imaging purposes, a time gating of 0−1 ns can provide an image selectively from species stained by epicocconone. This provides an additional advantage in its use in conjunction with other fluorescent markers like fluorescein, which have much longer lifetimes. Moreover, the fluorescence enhancement observed in micelles, with no spectral shift, is likely to be observed with membranes as well. Since protein-bound epicocconone has been reported to fluoresce with a considerable red shift, the fluorophore can possibly be used as a dual emitting stain, capable of imaging different subcellular components, without the need of multiplexing with other dyes.

Acknowledgment. This work is supported by CSIR Research Grant No. 01 (1851)/03/EMR-II. D.P. thanks the CSIR for a Junior Research Fellowship.

Supporting Information Available: Computational details and B3LYP/6-31G*-optimized geometry of epicocconone, in the form of Cartesian coordinates, total electronic energy, vertical excitations in different polar solvents, etc., along with other optimized structure and spectral and temporal data. This material is available free of charge via the Internet at http://pubs.acs.org.

References and Notes

(1) Mukherjee, P.; Fulton, D. B.; Halder, M.; Han, X.; Armstrong, D. W.; Petrich, J. W.; Lobban, C. S. *J. Phys. Chem. B* **2006**, *110*, 6359.
(2) Bell, P. J. L.; Karuso, P. *J. Am. Chem. Soc.* **2003**, *125*, 9304.
(3) Zhao, Y.; Zheng, Q.; Dakin, K.; Xu, K; Martinez, M. L.; Li, W.-H. *J. Am. Chem. Soc.* **2004**, *126*, 4653.
(4) Wang, L.; Cole, K. D.; Gaigalas, A. K.; Zhang, Y.-Z. *Bioconjugate Chem.* **2005**, *16*, 194.
(5) Mackintosh, J. A.; Choi, H.-Y.; Bae, S.-H.; Veal, D. A.; Bell, P. J.; Ferrari, B. C.; Van Dyk, D. D.; Verrills, N. M.; Paik, Y.-K.; Karuso, P. *Proteomics* **2003**, *3*, 2273.

(6) Coghlan, D. R.; Mackintosh, J. A.; Karuso, P. *Org. Lett.* **2005**, *7*, 2401.
(7) Goodwin, A. P.; Mynar, J. L.; Ma, Y.; Fleming, G. R.; Frechet, J. M. J. *J. Am. Chem. Soc.* **2005**, *127*, 9952.
(8) Badugu, R.; Sakamoto, K. *Chem. Commun.* **2003**, 1368.
(9) Mukherjee, T. K.; Ahuja, P.; Koner, A. L.; Datta, A. *J. Phys. Chem. B* **2005**, *109*, 12567.
(10) Panda, D.; Datta, A. *Chem. Phys. Lett.* **2006**, *426*, 100.
(11) Panda, D.; Mishra, P. P.; Khatua, S.; Koner, A. L.; Sunoj, R. B.; Datta, A. *J. Phys. Chem. A* **2006**, *110*, 5585.
(12) Panda, D.; Datta, A. *J. Chem. Phys.* **2006**, *125*, 054513.
(13) Becke, A. D. *J. Chem. Phys.* **1993**, *98*, 5648.
(14) Becke, A. D. *J. Chem. Phys.* **1993**, *98*, 1372.
(15) Pople, J. A.; et al. *Gaussian 03*; Gaussian, Inc.: Pittsburgh, PA, 2004.
(16) Wiberg, K. G.; Stratmann, R. E.; Frisch, M. J. *J. Chem. Phys.* **1998**, *297*, 60.
(17) Stratmann, R. E.; Scuseria, G. E.; Frisch, M. J. *J. Chem. Phys.* **1998**, *109*, 8218.
(18) Schaftenaar, G.; Noordik, J. H. *J. Comput.-Aided Mol. Des.* **2000**, *14*, 123.
(19) Mennucci, B.; Cances, E.; Tomasi, J. *J. Phys. Chem. B* **1997**, *101*, 10506.
(20) Roy, D.; Karmakar, R.; Mondal, S. K.; Sahu, K.; Bhattacharyya, K. *Chem. Phys. Lett.* **2004**, *399*, 147.
(21) Dwars, T.; Paetzold, E.; Oehme, G. *Angew. Chem., Int. Ed.* **2005**, *44*, 7174.
(22) Maiti, N. C.; Mazumdar, S.; Periasamy, N. *J. Phys. Chem. B* **1998**, *102*, 1528.
(23) Mishra, P. P.; Datta, A. *J. Phys. Chem. B* **2005**, *109*, 24225.
(24) Turro, N. J. *Modern Molecular Photochemistry*; W.A. Benjamin: London, 1978.
(25) Gehlen, M. H.; De Schryver, F. C. *Chem. Rev.* **1993**, *93*, 189.
(26) Ashby, K. D.; Das, K.; Petrich, J. W. *Anal. Chem.* 1**997**, *69*, 1925.
(27) Majumder, S. K.; Gupta, P. K. *Lasers Life Sci.* **2000**, *9*, 143.
(28) Patra, D.; Mishra, A. K. *Analyst* **2000**, *125*, 1383.
(29) Askari, M. D. F; Vo-Dinh, T. *Biopolymers* **2004**, *73*, 510.
(30) Pasternack, R. F.; Bustamante, C.; Collings, P. J.; Gibbs, E. J. *J. Am Chem. Soc.* **1993**, *115*, 5393.
(31) Collings, P. J.; Gibbs, E. J.; Starr, T. E.; Vafek, O.; Yee, C.; Pomerance, L. A.; Pasternack, R. F. *J. Phys. Chem. B* **1999**, *103*, 8474.
(32) Khazraji, A. C.; Hotchandani, S.; Das, S.; Kamat, P. V. *J. Phys. Chem. B* **1999**, *103*, 4693.
(33) Pal, S. K.; Datta, A.; Mandal, D.; Bhattacharyya, K. *Chem. Phys. Lett.* **1998**, *288*, 793.
(34) Lukeman, M.; Wan, P. *J. Am. Chem. Soc.* **2003**, *125*, 1164.
(35) Smirnov, A. V.; Das, K.; English, D. S.; Wan, Z.; Kraus, G. A.; Petrich, J. W. *J. Phys. Chem. A* **1999**, *103*, 7949.
(36) Urano, T.; Hamaguchi, H.; Tasumi, M.; Yamanouchi, K.; Tsuchiya, S.; Gustafson, T. L. *J. Chem. Phys.* **1989**, *91*, 3884.
(37) Reichardt, C. *Chem. Rev.* **1994**, *94*, 2319.
(38) Dean, J. A., Ed. *Lange's Handbook of Chemistry*, 163th ed.; McGraw-Hill: New York, 1987.
(39) Fu, Y.; Lakowicz, J. R. *Anal. Chem.* **2006**, *78*, 6238.
(40) Geddes, C. D.; Lakowicz, J. R. *Topics in Fluorescence Spectroscopy, Vol. 8, Radiative Decay Engineering*; Springer: New York, 2005.
(41) Mali, K. S.; Dutt, G. B.; Mukherjee, T. *J. Chem. Phys.* **2006**, *124*, 199901.
(42) Becker, R. S.; Freedman, K.; Lenoble, C. *J. Phys. Chem.* **1986**, *90*, 4334.
(43) Paradies, H. H. *J. Phys. Chem.* **1980**, *84*, 599.
(44) Berr, S. S.; Coleman, M. J.; Jones, R. R. M.; Johnson, J. S. *J. Phys. Chem.* **1986**, *90*, 6492.
(45) Zana, R. *J. Phys. Chem. B* **1999**, *103*, 9117.
(46) Grant, C. D.; Steege, K. E.; Bunagan, M. R.; Castner, E. W., Jr. *J. Phys. Chem. B* **2005**, *109*, 22273.
(47) Lala, A. K. *Chem. Phys. Lipids* **2002**, *116*, 177.